Remote Sensing of Environment 298 (2023) 113828

Contents lists available at ScienceDirect

Remote Sensing of Environment

journal homepage: www.elsevier.com/locate/rse

Monitoring selective logging intensities in central Africa with sentinel-1: A canopy disturbance experiment

Chloé Dupuis *, Adeline Fayolle, Jean-François Bastin, Nicolas Latte, Philippe Lejeune

TERRA Teaching and Research Centre (Forest is Life), Gembloux Agro-Bio Tech, University of Liege, Passage des Déportés n°2, 5030 Gembloux, Belgium

ARTICLE INFO

Edited by Dr. Marie Weiss

Keywords:
Logging intensity
Sentinel-1 SAR time series
Tropical forest degradation
UAV images
Central Africa

ABSTRACT

Forest degradation is a major threat to tropical forests, and effective monitoring using remotely sensed data is subject to significant challenges. In particular, consistent methods for detecting subtle changes in the forest canopy structure caused by selective logging are lacking. Here, using a unique dataset collected in southeastern Cameroon, covering over 22,000 ha of monthly harvesting areas, >6000 locations of harvested trees, and an independent canopy gap dataset developed from an uninhabited aerial vehicle flight (UAV; RGB camera) of approximately 1500 ha, a new method was designed to monitor canopy disturbance and logging intensity in Central Africa. Using Sentinel-1 synthetic aperture radar (SAR) data, the method was conceptualised using a two-step, two-scale approach, which better matched logging practices. First, (non-)harvesting activity areas were identified using textural indices at a spatial resolution of 300 m (step 1), and within these harvesting activity areas, canopy gaps were detected at a resolution of 10 m (step 2). Both steps were based on monthly differences in the Sentinel-1 SAR time series computed using the average of the 12 months preceding and the average of the three months following the month of interest. This method identified harvesting activity areas (step 1 at 300 m resolution) of over 12,004 km^2 with high accuracy (omission and commission errors for both classes ≤0.05) and, within them, detected canopy gaps (step 2 at 10 m resolution) with a global accuracy of 0.89. Although some canopy gaps were subject to omission and commission errors (0.39 and 0.05, respectively), this method yielded better results than other available approaches. Compared to the UAV canopy gaps, this method detected most of the small gaps (≤ 500 m^2), which represent 80% of all disturbed areas, whereas other available approaches missed at least 70% of these and consequently missed most of the disturbance events occurring in a selectively logged forest. Furthermore, the predictions were correlated with logging intensity, *i.e.*, the number of trees and volume cut per hectare, which are two important criteria for assessing the sustainability of logging activities. This two-step two-scale method for short-term, monthly monitoring of logging disturbances and intensity has strong practical implications for forest administration and certification bodies in Central Africa.

1. Introduction

Tropical forests are threatened by human activities, and their area has decreased by 17% since 1990, with at least 10% of the remaining forests being degraded (Vancutsem et al., 2021). Forest degradation is caused by anthropogenic disturbances including logging, mining, road construction, agriculture, fires, and wood fuel harvesting (Pearson et al., 2017; Tyukavina et al., 2018). The frequency and intensity of these disturbances determine how quickly a degraded state is reached and the time required for forest recovery (Ghazoul et al., 2015; Rutishauser et al., 2015). Tropical forest degradation is estimated to be responsible for 2.06 Gt CO_2 yr^{-1} of carbon emissions (Pearson et al., 2017) and approximately 20% of tropical forests are disturbed by logging activities that can subsequently lead to forest degradation (Hosonuma et al., 2012; Hubau et al., 2020). In the context of the new European law addressing deforestation and degradation free products, forest degradation is defined as "harvesting operations that are not sustainable and cause a reduction or loss of the biological or economic productivity and complexity of forest ecosystems, resulting in the long-term reduction of the overall supply of benefits from forest, which includes wood, biodiversity and other products or services" (European Commission, 2021).

In Central African tropical forests, approximately 53.4 million hectares are used under logging concessions, of which 10% are certified by the Forest Stewardship Council (BAD, 2018; FSC, 2022).

* Corresponding author.
E-mail address: chloe.dupuis@uliege.be (C. Dupuis).

https://doi.org/10.1016/j.rse.2023.113828
Received 24 November 2022; Received in revised form 15 September 2023; Accepted 20 September 2023
Available online 26 September 2023

Management planning by logging companies includes dividing their land into different zones and then moving the location of activities from year to year and month to month (BAD, 2018). Logging is highly selective in the region with a limited number of high-value tree species targeted, and a restricted number of cut trees (0.7–4.0 trees.ha^{-1}) every 20–35 years (BAD, 2018; Medjibe et al., 2011). In addition to felling gaps caused by cut trees, skid trails, logging roads, and log yards built for the extraction and storage of logs also contribute to forest disturbances. Thus, logging practices result in changes in forest cover that are different from other land-use activities, such as mining, road construction, agriculture, fires, and wood fuel harvesting (Pearson et al., 2017; Tyukavina et al., 2018), and occur on two scales. On a landscape scale, active logging front harvesting activity areas are visible and can be detected using satellite data, *e.g.*, logging roads are visible on the forest cover loss maps by Hansen et al. (2013). On a smaller scale, dotted and sparse patches of felling gaps and linear aspects of roads and trails appear in the canopy cover, *e.g.*, in Landsat and SPOT images (De Wasseige and Defourny, 2004).

Today, there is no transparent, systematic, and robust ground-based assessment of the state of forest degradation caused by logging activities, especially in Central Africa, where forest disturbances occur on a smaller scale than on other continents, mainly because of a low logging intensity (1–4 trees.ha^{-1}) (Durrieu de Madron et al., 2000) in comparison to that in South-East Asia (Sist et al., 1998) and South America (Sist and Ferreira, 2007) (15–18 trees.ha^{-1}). Recent developments in remote sensing data acquisition, processing capacity, and available tools offer new opportunities to monitor forest disturbances (Jackson and Adam, 2020; Sanchez-Azofeifa et al., 2017) and high-resolution (*i.e.*, spatial resolution between 10 and 30 m) optical data can be used to monitor forest degradation (Hethcoat et al., 2019; Hirschmugl et al., 2017; Mitchell et al., 2017). For example, in the Amazon, the use of multitemporal data and spectral mixture analysis enabled the detection of degradation and natural disturbances every two years using Landsat images (resolution = 30 m; producer accuracy = 0.44; user accuracy = 0.73) (Bullock et al., 2020). In addition, a machine learning method allowed the detection of highly selective logging ($<$ 15 m^3.ha^{-1}; 1–2 trees.ha^{-1}) on a local scale (11,000 ha) in the Brazilian Amazon using Landsat images (Hethcoat et al., 2019). Globally, the Joint Research Centre (JRC) of the European Commission has produced annual pantropical degradation maps using Landsat images, regardless of the cause of disturbance (Vancutsem et al., 2021).

However, optical imagery has limitations such as dependency on cloud-free images, which are particularly rare in several areas of Central Africa (King et al., 2013), and the influence of sun-scene-sensor geometries (Ploton et al., 2017) preventing regular monitoring. To overcome these limitations, several studies have shown that synthetic aperture radar (SAR) data can be used to monitor forest disturbances because microwave remote sensing systems are less influenced by weather conditions (Mermoz et al., 2015). Long wavelengths (L-band, $\lambda \sim 23$ cm and P-band, $\lambda \sim 65$ cm) are particularly suitable for use in tropical forests because of their better vegetation canopy penetration (Deutscher et al., 2017). ALOS-2 PALSAR-2 data (L-band, revisit time 14 days) were used to detect early-stage deforestation sites in Peru and Brazil where felled trees were left on the ground (Watanabe et al., 2018). ALOS-2 PALSAR-2 data have also been used in the JJ-FAST system to detect forest disturbances in the tropics, but with a minimum mapping unit (MMU) of 2 ha which is not adapted to the degradation process that occurs on a finer scale (Nagatani et al., 2018). The upcoming BIOMASS satellite, the first P-band SAR space mission (Scipal et al., 2010), is expected to significantly advance forest ecosystem monitoring. However, its temporal resolution (twice a year) presents limitations for near-real-time monitoring of logging activities.

The deployment of Sentinel-1 satellites in 2014 by the European Space Agency provided a global source of free C-band SAR data. With a revisit time of 12 days over the tropics and a spatial resolution of 10 m, it offers the opportunity to systematically monitor the degradation of tropical forests on a large scale. Because the shorter microwave wavelengths in the C-band (5.6 cm) have limited penetration into dense forest canopies, C-band backscatter measurements provided by Sentinel-1 SAR are not suitable for monitoring tropical forest biomass. However, the dense time series and high spatial resolution of Sentinel-1 SAR data make measurements sensitive to changes in the canopy structure and suitable for detecting small or narrow patches of disturbance (Hethcoat et al., 2021; Reiche et al., 2021). Recently, several studies used Sentinel-1 SAR data to monitor tropical forest disturbances, including those caused by logging. In French Guiana, the detection of high logging intensity forest exploitation (25 m^3.ha^{-1}) with a MMU of 0.2 ha achieved a user accuracy of 0.95 and a producer accuracy of 0.37 when validated using optical data (Ballère et al., 2021). In the Brazilian Amazon, the use of time series and textural indices was also efficient (Hethcoat et al., 2021) but only when the logging intensity was high ($>$ 20 m^3.ha^{-1}). The Radar for Detecting Deforestation (RADD) alert system provides pantropical near-real-time monitoring of all types of disturbances, with an MMU of 0.1 ha (Reiche et al., 2021). While these studies marked significant advancements in detecting forest disturbances using Sentinel-1 SAR data, they may not be fully suitable for the specific context of selective logging in Central Africa, which is characterised by low logging intensities ($<$ 15 m^3.ha^{-1}) and small felling gaps ($\sim$ 300 m^2) (Medjibe et al., 2011). Recently, Sentinel-1 SAR shadows were used to detect canopy gaps caused by logging in Gabon and the method was calibrated using uninhabited aerial vehicle (UAV) LiDAR data (Carstairs et al., 2022). While this study was based on a small local data set (261 canopy gaps over 310 ha), the use of UAV LiDAR data allowed refining the comprehension of gap detection using Sentinel-1 SAR data, which was an innovation in the field. However, there is an urgent need to bridge the gap between ground- and satellite-based measurements. First, accuracy assessment without robust field data has not received much attention and remains an issue in the report of selective logging detection (Hethcoat et al., 2021). Second, integrating field data with canopy opening estimates from existing systems (Carstairs et al., 2022; Reiche et al., 2021) is essential for generating metrics specific to the forestry sector, such as the number of trees and volume of timber harvested per hectare (Welsink et al., 2023).

To address the need for effective monitoring of selective logging, specifically adapted to detect harvesting activities and canopy gaps in Central Africa, a robust method must be developed. This method must be able to monitor disturbances caused at low logging intensity ($<$ 15 m^3.ha^{-1}) over short time periods to gain a complete understanding of the role of forest logging activity in forest degradation. To this end, the two-step two-scale approach proposed in this study was designed to fit logging activities in Central Africa, detecting harvesting activity areas and canopy gaps at 300 m and 10 m resolutions, respectively, on a monthly basis. The approach was calibrated and validated in a unique field experiment, and optical images and digital model surfaces from UAV flights were used to depict forest logging activities in detail. The capacity of the method to not only locate forest disturbances but also predict logging intensity in terms of the number and volume of trees cut per hectare was evaluated, which are two criteria commonly used by the forestry sector to assess the sustainability of logging and plan activities. Finally, the results obtained in this study were compared with available large-scale approaches, that is, the JRC map (Vancutsem et al., 2021) and the RADD system (Reiche et al., 2021).

2. Material and methods

2.1. Field and satellite data collection and processing

2.1.1. Field data

The study area covers 12,004 km^2 in southeastern Cameroon and is centred on the Forest Management Units (FMUs) granted to the FSC-certified Pallisco-CIFM company. These forests are semi-deciduous *Celtis* forests (Fayolle et al., 2014; Réjou-Méchain et al., 2021). In Central

Africa, FMUs are divided into annual cutting areas, which are in turn divided into monthly harvesting activity areas. Logging roads are built one year before the planned logging operations in the annually cut areas. During the year of harvesting operations, the logging front advances through predefined harvesting activity areas monthly. The logging company archives spatial data on harvesting areas, including the corresponding month of operation and the locations of log yards, logging roads, skid trails, and cut trees. These data were used to build a reference dataset at two spatial scales, harvesting activity areas and canopy gaps (Fig. 1a and d). The data were collected in the field with a GPS and then checked and readjusted by a cartographer who geolocated all skid trails down to the stumps of cut trees and repositioned the trees at the end of each skid trail. The species and the 10 cm wide diameter class of each tree were also recorded. The volume of cut trees was estimated from the midpoint of the diameter class using species-specific allometric equations (Table S1). According to these data provided by the logging company, the average logging intensity was estimated to be 16 $m^3.ha^{-1}$ and 1.6 $trees.ha^{-1}$.

2.1.2. UAV flights

Two sets of uninhabited aerial vehicle (UAV) data (RGB images) were acquired (Table S2) after timber harvesting in May 2019 and May 2021, covering two distinct harvesting areas of 504 ha and 964 ha, respectively. High-precision RTK/PPK GPS was used to ensure correct georeferencing of the images. Orthophoto mosaicking and a digital surface model (DSM) at 10-cm resolution were generated using *Metashape* software (Lisein et al., 2013). All canopy gaps visible in the orthophotos and DSM were manually digitised (n = 1384) and categorised into felling gaps, roads, skid trails, log yards; the category other was used when the cause was not clearly identifiable. Felling gaps were identified and distinguished from natural ones owing to their distinct patterns, which included a crown, a straight cut, a hole where the log

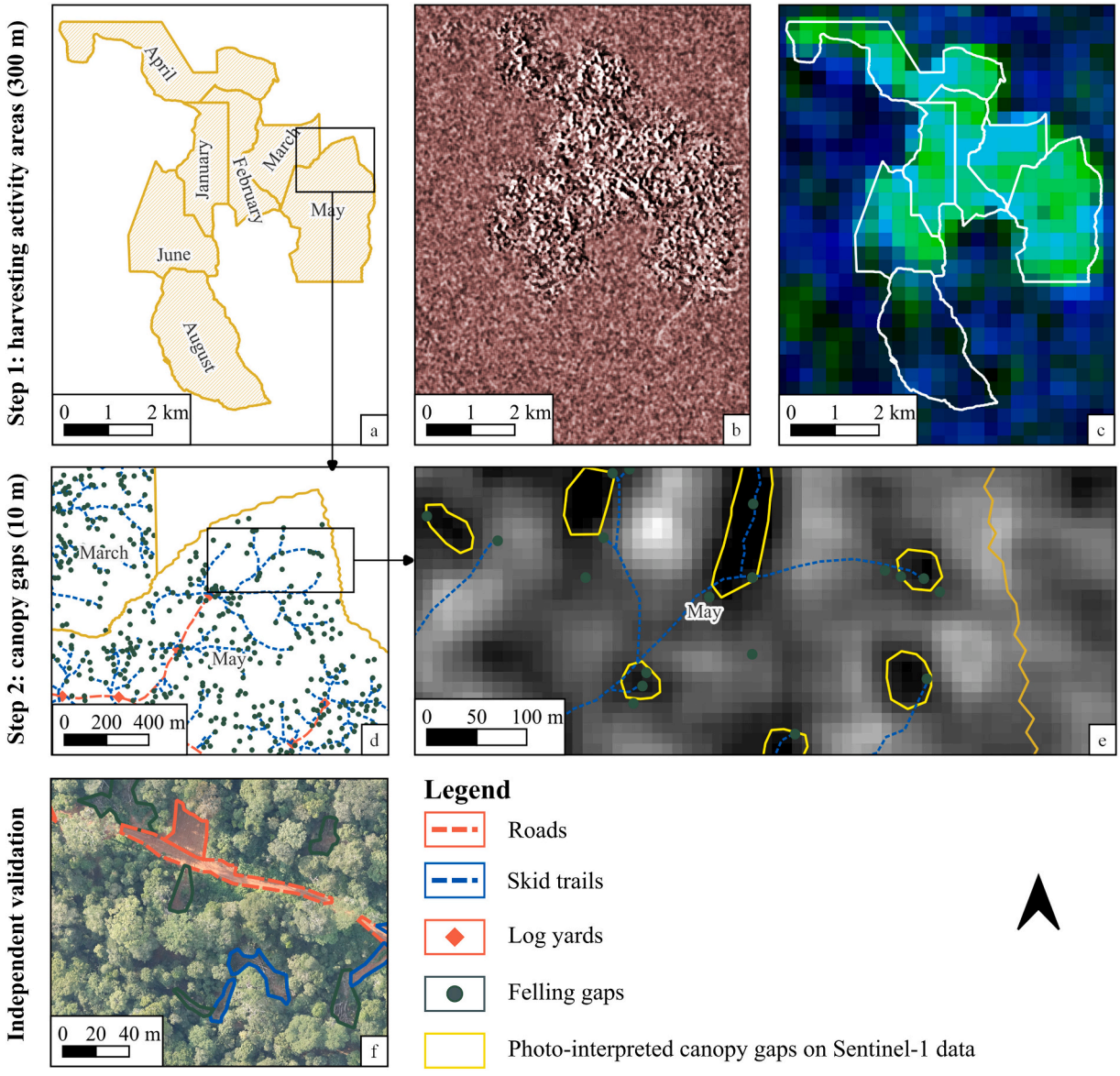

Fig. 1. Data used in this study for the detection of (non-)harvesting activity areas at 300 m resolution in step 1 (a–c), and of the canopy gaps at 10 m resolution in step 2 (d–e) and for the independent validation using UAV images taken after logging (f). (a) and (d) spatial data provided by the logging company for the annual cutting area 2019; (b) red-coloured grey composition of VH-diff, VV-diff and VH:VV ratio for May 2019; (c) textural indices at 300 m resolution for May 2019; (e) canopy gaps photo-interpreted on Sentinel-1 SAR data (here VH-diff) with the help of spatial data provided by the logging company; (f) UAV image and photo-interpreted canopy gaps for May 2019. Extent of the ACA 2019 (a): 423469, 362361: 430647, 370982 (EPSG: 32633). (For interpretation of the references to colour in this figure legend, the reader is referred to the web version of this article.)

was removed, and ideally, a stump (Fig. S1). The UAV canopy gap dataset built from the photo-interpretation of logging disturbances was used to independently validate the method (Fig. 1f).

2.1.3. Satellite data and processing

Sentinel-1 (VH and VV, C-band) Ground Range Detected (GRD) products acquired in interferometric wide mode and in descending orbit were obtained from the Google Earth Engine. All scenes between 2016 and 2021 were used, with a revisit time of 12 days for the study area. A set of data treatments was applied in Google Earth Engine using the European Space Agency Sentinel-1 Toolbox, including the application of an orbit file, removal of thermal noise, removal of GRD border noise, radiometric calibration to sigma naught, and range-Doppler terrain correction. In addition, a radiometric slope correction was applied and the data were transformed to gamma naught which is better adapted for dense forests (Rudant and Frison, 2019), using codes developed previously (Vollrath et al., 2020). Multitemporal speckle filtering (3 × 3 pixels window) was then applied (Quegan and Yu, 2001). Subsequently, for each band (VH and VV) and date, the values were divided by the median of the values within the concession boundaries. This correction facilitated image comparison between different dates and highlighted non-forested pixels. A set of standardised VV- and VH-polarised backscatter images with a resolution of 10 m was generated for the entire area of interest. Finally, for each month, the difference between the average of the 12 months of data before and the average of the three months after the month of interest was calculated (Fig. 2). Using one year of data before the month of interest allowed smoothing of seasonal variability over the entire year. Using three months of data after the month of interest was found to be a good compromise between a stabilised and reactive signal and avoided the dilution of the signal generated by the canopy disturbance, as understory vegetation quickly reappears. The final output differences in the VH (VH-diff) and VV (VV-diff) bands were generated for each month between 2017 and 2021 (Fig. 1b Fig. 2).

2.2. Detection of harvesting activity areas and canopy gaps

With the aim of fitting logging activities in the field and providing a tool that can be directly used by the forestry sector in Central Africa, particularly to estimate logging intensity which is evaluated on the scales of harvesting activity or an annual cutting area, a detection method divided into two steps on two spatial scales was developed (Fig. 2): (1) the detection of harvesting activity areas with any signs of logging activities per 300-m grid cell, and (2) within these harvesting activity areas, the detection of 10-m disturbed pixels in which wood was extracted, called canopy gaps.

2.2.1. Predictor variables

Several predictor variables were tested at each step of the method (Fig. 1c and 2). Local statistics and Haralick features were calculated based on VH-diff using applications in *Orfeo ToolBox,* within a 31-pixel window for step 1 and within a 5 pixels size window for step 2 (Haralick et al., 1973). Only cross-polarised observations (VH bands) were used because they are recognised to be better for tracking forest degradation and identifying changes from volumes (forest) to surfaces (non-forest) (Kellndorfer, 2019). In the first step, the exposition and slope based on the SRTM as predictor variables were also tested, as well as the month, because the variation in humidity between wet and dry seasons can influence the SAR data (Flores-Anderson et al., 2019). These variables were averaged at a resolution of 300 m. In the second step, VV-diff, VH-diff, and the ratio of VH-diff to VV-diff were tested. Among these, the best explanatory variables were selected using the *VSURF* package in R (Table S1). The *VSURF* method is based on random forests; preliminary ranking of the explanatory variables is obtained using the importance indicator of the random forest, followed by a stepwise ascending variable introduction strategy to highlight the most important variables (Genuer et al., 2014). The second subset of variables of *VSURF* which aims to minimise redundancy while focusing on a prediction objective was used. Finally, 26 and 7 variables were selected for the first and second steps, respectively (Table S3).

2.2.2. Training and test datasets

To detect harvesting activity areas at a resolution of 300 m (step 1), spatial information provided by the logging company was used to build a reference dataset (Fig. 1a). References for the harvesting activity areas corresponded to the boundaries of the monthly harvesting areas logged between 2017 and 2021. For non-harvesting areas, annual cutting areas planned to be logged after 2025 were used. The training and test pixels were chosen to be distributed in time and space through the logging concession, and were spatially independent (Table S4). In total, 9002 pixels of 300 × 300 m were used in the reference dataset, with 80% used for training and 20% for validation.

To build a reference dataset for the detection of canopy gaps at a 10-m resolution (step 2), VH-diff and VV-diff were photo-interpreted with the help of spatial data from the logging company (*i.e.*, location of cut trees, log yards, and skid trails) for 2019 and 2020 (Fig. 1d). One operator checked the spatial data from the logging company, following every skid trail to the tree stumps to guide the photo-interpretation of the SAR data using VH-diff and VV-diff, on which canopy gaps were visible, to create a reference dataset (Fig. 1e). Although the utilisation of spatial data from the company helped guide the operator's assessment during the photo-interpretation of Sentinel-1 SAR data, it is important to acknowledge that this approach has some limitations. Some canopy gaps may have been overlooked or missed during the interpretation. In total, 801 polygons corresponding to canopy gaps created between January 2019 and August 2020 were digitalised, with a mean size of 1538 m^2 and minimum and maximum sizes of 362 m^2 and 5802 m^2, respectively (Fig. 1e). In the harvesting activity areas, 80% of the polygons were used for training and 20% for testing, which amounts to 24,566 10 × 10 m pixels for the "canopy gaps" class. The same number of pixels was randomly selected in annual cutting areas planned to be logged after 2025 to build the reference dataset for the "forest" class. The training and test datasets were spatially and temporally distributed (Table S5).

2.2.3. Model building and validation

Two random forest classification models were built in R (*randomForest* package) to detect (1) harvesting activity areas in a 300-m grid and (2) canopy gaps in 10-m pixels (Fig. 2). The number of trees used in each model was set to 2000 and three, respectively, and two predictor variables were used at each node for the two steps based on the Gini index. Additional treatments were applied to improve the predictions of random forest models. For the detection of harvesting activity areas (step 1), predictions with an area >180 ha were maintained, which corresponded to the minimum surface of the monthly harvesting area at the study site. Then, the false positives were reduced by validating the predictions with the month after and by retaining only the pixels detected twice. The results from step 1 were used as a mask inside which canopy gaps were detected in 10-m pixels (step 2). As the "canopy gaps" class had a halo of false positives compared to the reference dataset, only predictions with a confidence rate > 0.95 were retained. Finally, predictions <500 m^2 were removed (MMU of 500 m^2) for two reasons: (1) to improve the intersection over union (IoU, area of overlap/area of union) between the predictions and rasterised UAV canopy gaps (see Section 2.3.), and (2) to adhere to the limit imposed by the IW GRD high-resolution product with a spatial resolution of 20 × 22 m (ESA, 2022). Thus, the MMU served as a post-processing step that can be adjusted as needed. A confusion matrix based on the test datasets was built for the two steps to control the user and producer accuracies.

2.2.4. Logging intensity prediction

To establish if this method could be used to monitor logging intensity, linear regression between the percentage of canopy gaps area

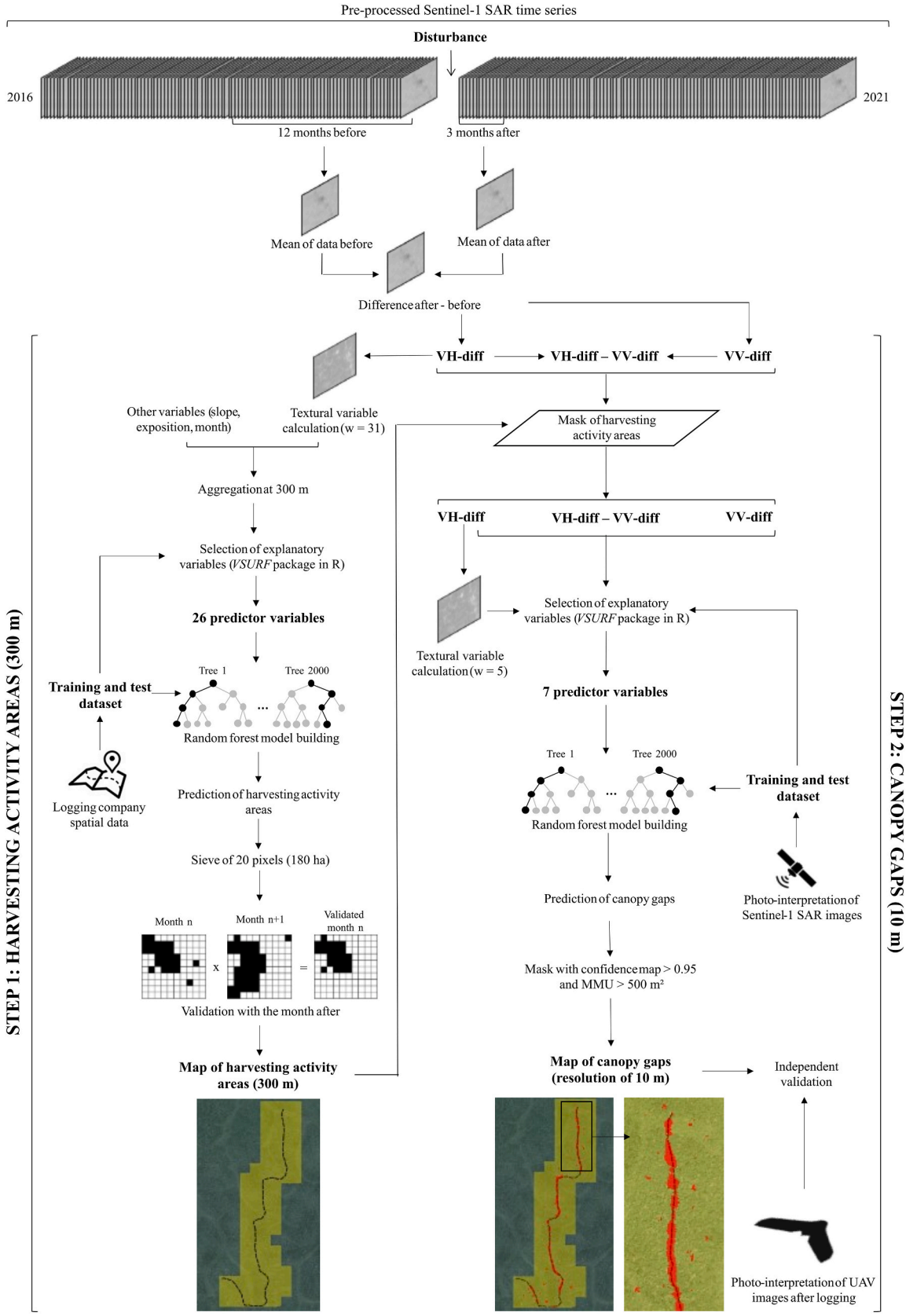

Fig. 2. Flowchart of the two step two scale method implemented to monitor canopy disturbance in the tropical forest caused by selective logging using Sentinel-1 SAR time series. In the first step (left), harvested activity areas (in yellow) were identified at 300 m resolution, inside which canopy gaps (in red) were identified at 10 m resolution in the second step (right). (For interpretation of the references to colour in this figure legend, the reader is referred to the web version of this article.)

predicted and both the number and volume (m^3) of cut trees inside grids between 100 and 2000 m of side length were established. The adjusted R-squared value, root mean squared error (RMSE), standard error (SE), and mean absolute error (MAE) were calculated from these relationships. Monthly canopy gap predictions correspond to skid trails and felling gaps because roads and log yards were built before the month of harvesting in this concession. To assess which types of disturbance were most related to logging intensity, the same relationships between UAV-based photo-interpreted canopy gaps were divided into three categories (felling gaps and skid trails, felling gaps, and all gaps), and both the number and volume of cut trees were established.

2.3. Independent validation and comparison using available approaches

The UAV-based photo-interpreted canopy gaps were used as an independent validation dataset to compare the quality of the canopy gap detection using this method with the other available approaches, namely the RADD system (Reiche et al., 2021) and the JRC map (Vancutsem et al., 2021). The UAV canopy gaps were rasterised based on the extent and resolution (10 m) of the predictions for comparison. Predictions were considered correct if they intersected rasterised UAV canopy gaps. The proportion of predictions that were correct (user accuracy) and the proportion of UAV canopy gaps that were well detected (producer accuracy) using the surfaces of the predictions were calculated. The producer accuracy was calculated for each type of canopy gap (*i.e.*, felling gaps, skid trails, roads, log yards, and others) and evaluated by applying different thresholds (up to 2300 m^2) to the UAV canopy gaps. Finally, the IoU between the predictions and rasterised UAV canopy gaps was calculated for the three methods to estimate how well the predictions matched actual ground data.

3. Results

3.1. Detection of harvesting activity areas and canopy gaps

The method showed a global accuracy of 0.98 and 0.89 for the detection of harvesting activity areas and canopy gaps, respectively, based on test datasets. Considering the predictor variables used in the random forest model for the detection of harvesting activity areas (step 1), the variance in VH-diff, calculated with a 31-pixel window, was the most important variable (Fig. S2). The confusion matrix of the final classification for this step showed that harvesting and non-harvesting activity areas were well discriminated with user and producer accuracies $\geq$0.95 (Table 1). For the detection of canopy gaps (step 2), the most important predictor variables in the random forest model were VH-diff, the variance of VH-diff, and the mean of VH-diff, calculated with a five-pixel window (Fig. S3). The detection of canopy gaps was good, with no commission errors, but some pixels were omitted (producer accuracy = 0.78, Table 1) and classified as forest areas (user accuracy for forest areas = 0.82, Table 1).

3.2. Estimation of logging intensity

The percentage of the canopy gap area detected by this method was compared to the logging intensity, and the strength of the relationships increased (higher adjusted R^2 and lower RMSE) with the aggregation scale considered for both volume (Fig. 3) and the number of trees cut per hectare (Fig. S4). The adjusted R^2 increased with the grid size (Fig. 4), and a resolution of 200 m emerged as a suitable threshold, beyond which the relationships became less noisy, with an adjusted $R^2 > 0.5$ (Fig. S4, Fig. 3). Monthly predictions corresponding to skid trails and felling gaps were used because these types of gaps showed the highest correlation with logging intensity, as indicated by the relationships derived from the UAV canopy gaps (Fig. S5). The relationships for volume harvested per hectare were slightly better than those for the number of trees harvested per hectare (Fig. 4), whereas the opposite was observed for relationships based on UAV canopy gaps (Fig. S5). Logging can be very intense locally (up to 9 trees and 200 $m^3.ha^{-1}$ for a 100-m grid); however, this restricted pattern is due to the local density of exploited trees and is smoothed at larger grid size (< 2 trees and 30 $m^3.ha^{-1}$, with the majority <20 $m^3.ha^{-1}$ for a 2000-m grid). In contrast, the RADD system (Reiche et al., 2021) and the JRC map (Vancutsem et al., 2021) were less effective in predicting logging intensity (Fig. 4, Fig. S6 to S9).

3.3. Independent validation and comparison with available approaches

Compared to rasterised UAV canopy gap areas, this method detected 61% of the canopy gaps, whereas the JRC and RADD systems detected only 28% and 20% of the canopy gaps, respectively. Regarding the precision of the three methods based on the UAV canopy gaps, the commission errors were low (5%, 12%, and 2% for our method, the JRC map, and the RADD system, respectively); however, the RADD system and, to a lesser extent, the JRC map predicted only 62 and 124 polygons in the study area, respectively, in comparison to the 476 polygons detected by this method. An example of the predictions of the JRC map and RADD system is shown for the harvesting activity area in May 2019 (Fig. S10). IoU was low for all three methods ($0.33.10^{-3}$, $0.31.10^{-3}$, and $0.24.10^{-3}$ for this method, the JRC map, and the RADD system, respectively). The predictions obtained using this method slightly overestimated the canopy gap area (halo effect), whereas the other two methods overestimated the area but missed many small gaps (Fig. 5a and Fig. S10).

The size of the canopy gaps strongly influenced the detection performance; the larger the gaps, the better they were detected by the three methods, with a better performance of this method overall, particularly for smaller gaps (Fig. 5a). The UAV canopy gaps had a median size of 247 m^2 and the majority were < 500 m^2 (Fig. 5a). When considering gaps under 500 m^2, producer accuracy for this study ranged from 0.32 to 0.50, for the RADD system from 0.12 to 0.16, and for the JRC map from 0.19 to 0.26 (lines with triangles in Fig. 5a). When considering gaps >500 m^2, producer accuracy improved for the three methods, ranging from 0.74 to 1.00 for this study, from 0.28 to 0.69 for the RADD system and from 0.37 to 1.00 for the JRC map (dotted lines in Fig. 5a).

The type of canopy gap was also explored. Of the 3.88% canopy loss caused by logging activities (the proportion of UAV canopy gaps in the surveyed area), felling gaps were the most significant, accounting for 68% of the disturbed area. The detection performance varied with the type of logging disturbance for the three methods (Fig. 5b). However, for each type of disturbance, this method performed better than the JRC map and RADD system. The difference was particularly clear in the

Table 1
Confusion matrix for the detection of harvesting activity areas in a 300-m grid (step 1) and 10-pixel canopy gaps (step 2).

Step 1: harvesting activity areas (300 m)					**Step 2: canopy gaps (10 m)**				
		Reference					Reference		
		Forest	**Harvesting activity**	**User accuracy**			**Forest**	**Canopy gaps**	**User accuracy**
Prediction	**Forest**	483	21	0.95	Prediction	**Forest**	2516	549	0.82
	Harvesting activity	0	411	1		**Canopy gaps**	0	1995	1
	Producer accuracy	1	0.95	0.98		**Producer accuracy**	1	0.78	0.89

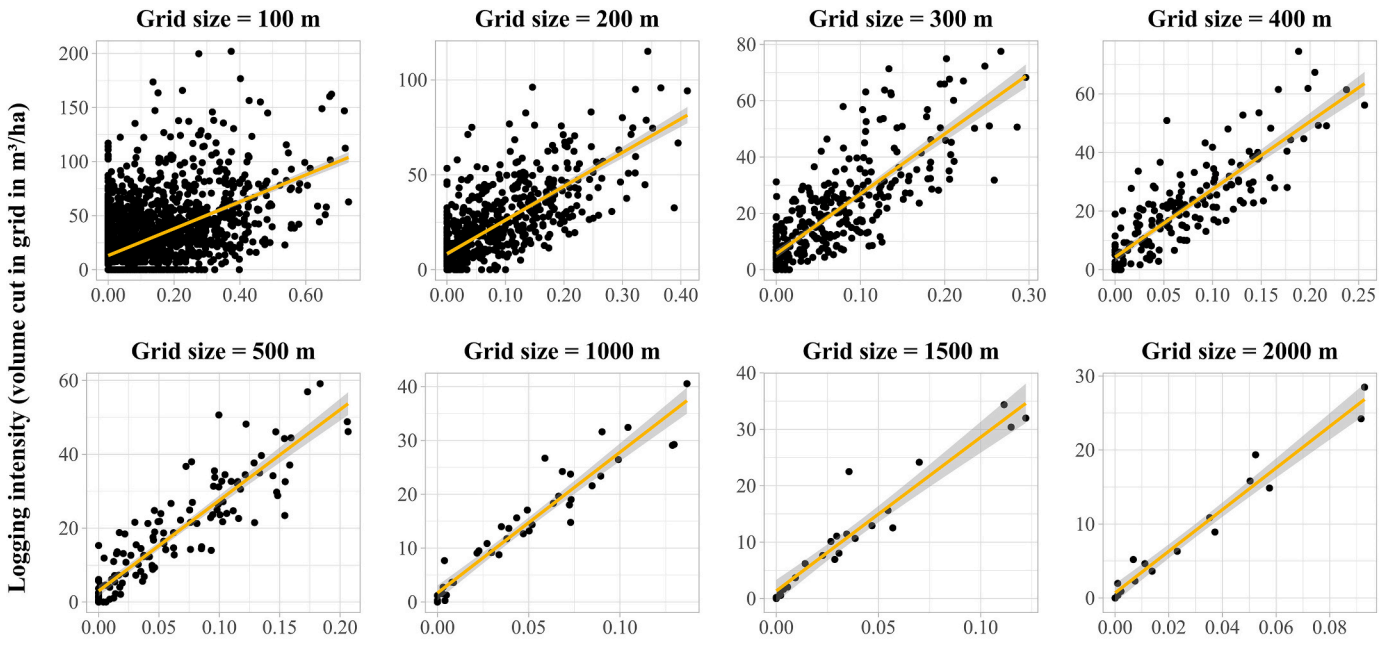

Grid size	a	b	SE of a	SE of b	Adj. R²	RMSE	MAE
100	13.09	124.32	0.54	3.73	0.30	23.64	17.35
200	8.37	177.79	0.66	6.17	0.54	13.34	10.14
300	5.64	212.94	0.79	8.64	0.64	10.30	7.87
400	4.28	231.38	0.83	9.82	0.74	8.05	6.02
500	3.00	245.42	0.73	9.61	0.82	6.10	4.62
1000	1.68	261.39	0.69	11.77	0.92	3.12	2.32
1500	1.35	272.44	0.95	18.22	0.91	3.15	1.98
2000	0.70	281.10	0.58	13.97	0.96	1.74	1.32

Fig. 3. Relationships between the logging intensity (volume of trees cut per hectare in a grid cell) and the percentage of canopy gap area detected by our method in the same grid cell by grid size. The table shows the results of linear regressions fitted for all grid sizes: the slope (a), the intercept (b), the standard error (SE) associated with a and b, the adjusted R^2 (Adj. R^2), the root mean squared error (RMSE), and the mean absolute error (MAE) in m^3 per hectare.

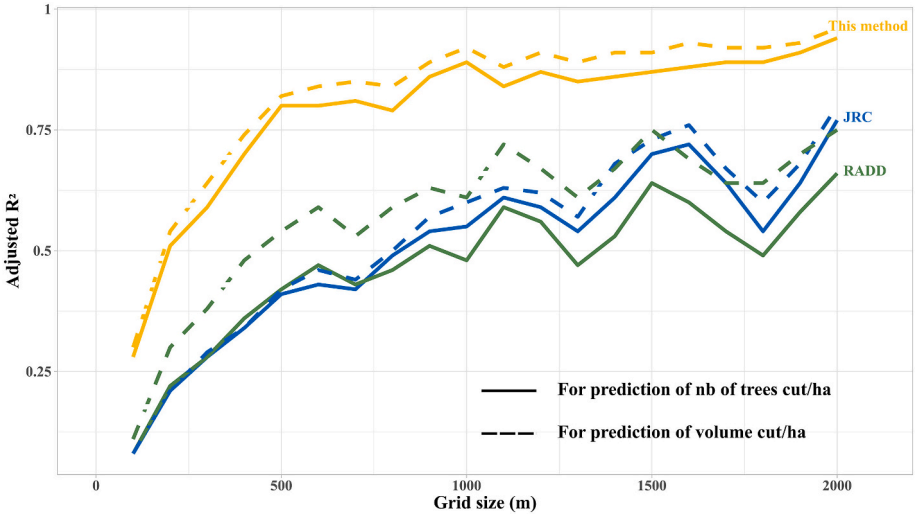

Fig. 4. Comparison of the performance of the three methods (this method, the RADD system and the JRC map) to estimate logging intensity (in terms of number of trees and volume cut per hectare) depending on observation scale. The adjusted R^2 of linear relationships between predicted logging intensity and logging intensity from the field according to grid size was computed for the different methods comparing this method (Fig. 3 and Fig. S4), the RADD system (Fig. S6 and S8) and the JRC map (Fig. S7 and S9).

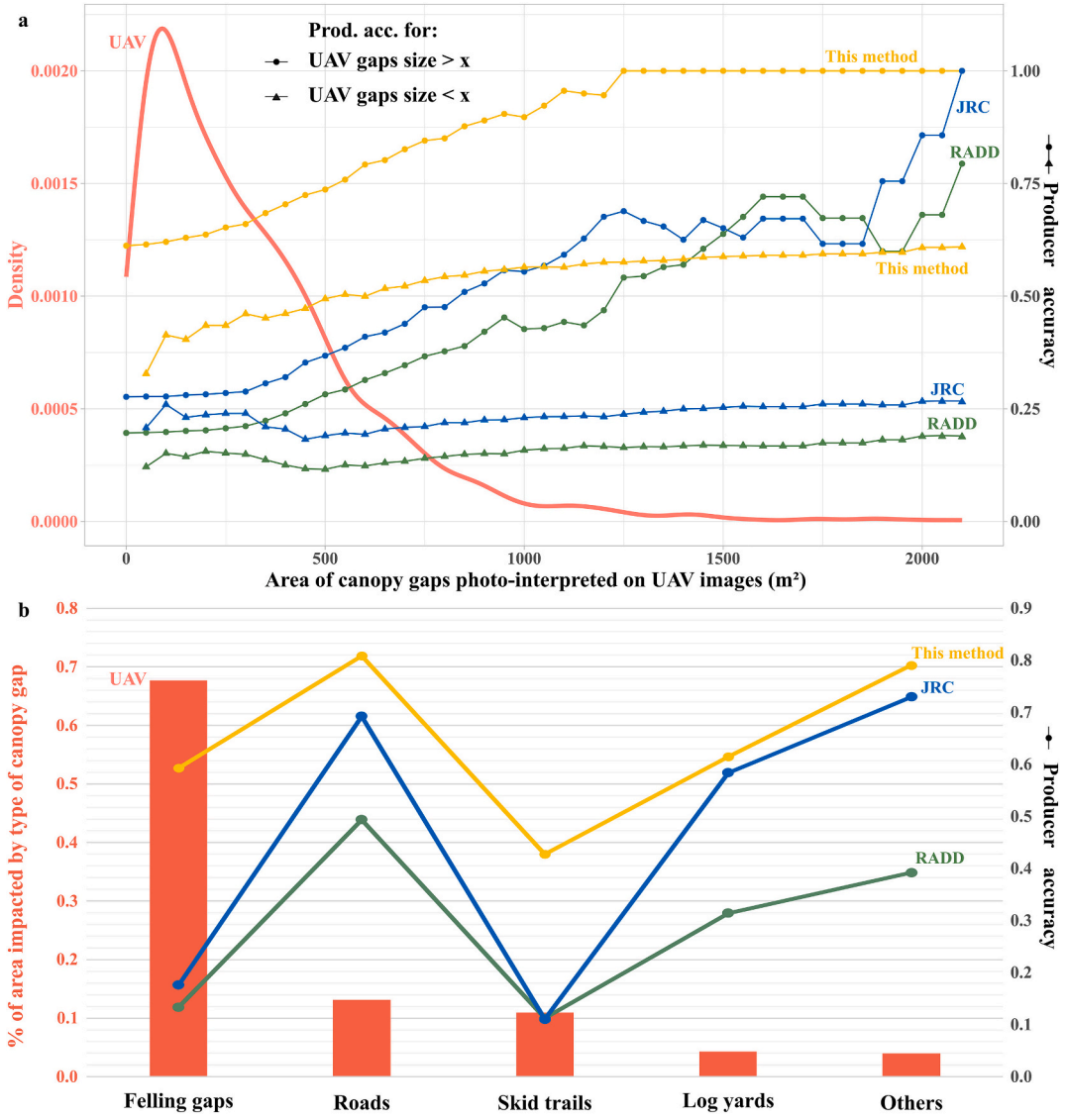

Fig. 5. Comparison of the performance of this method (in yellow) and that of other available approaches (the RADD system and JRC, in green and blue, respectively) when confronted with an independent dataset derived from the photo-interpretation of UAV images (in red). Specifically, performance to detect the disturbance events according to their size (a) and type (b) were examined. In a), the distribution of UAV photo-interpreted canopy gaps (left y axis = Density *i.e.*, the relative likelihood of gap size value within a specific interval) by gap size, and evolution of producer accuracy of the RADD system, JRC map, and this study (right y axis = Producer accuracy) by the area of UAV canopy gaps (x = area of UAV canopy gaps in m^2). In b), the distribution of impacted canopy cover by the type of logging disturbance (felling gaps, roads, skid trails, log yards, and others) using UAV canopy gaps and producer accuracy for this study, the RADD system, and the JRC map. (For interpretation of the references to colour in this figure legend, the reader is referred to the web version of this article.)

detection of felling gaps, for which the producer accuracy reached 0.59 and only 0.13 for the RADD system and 0.18 for the JRC map (Fig. 5b). The best detection performance was achieved for logging roads (producer accuracy = 0.81 in this study) and the worst for skid trails (producer accuracy = 0.43 in this study) (Fig. 5b).

4. Discussion

In this study, a two-step, two-scale method was developed for short-term and monthly monitoring of canopy disturbances in tropical forests, specifically fitted for logging practices in Central Africa. A unique combination of field datasets was used, including the location of monthly harvesting areas (> 22,000 ha) over five years, harvested trees (> 6000), and UAV images taken after logging (~ 1500 ha). This was possible because of the long-term partnership with the logging company. Monthly monitoring of harvesting activity areas at a 300-m resolution (step 1) and canopy gaps at a 10-m resolution (step 2) allowed the detection of the most common small-scale disturbance events and the estimation of logging intensity. Because of the completely independent validation based on after-logging UAV images that were photo-interpreted, the performance of this method was compared to that of other available approaches, the RADD system (Reiche et al., 2021), and the JRC map (Vancutsem et al., 2021), both of which were outperformed.

The proposed method showed good results in detecting selective logging activities in the study area (12,004 km^2) where semi-deciduous forests dominate the landscape (Fayolle et al., 2014; Réjou-Méchain et al., 2021). The excellent detection performance of the harvesting activity area at a 300-m resolution (step 1) is a real asset of the method, particularly because the predictions were highly accurate (low commission error), which is important for monitoring systems (Reiche et al., 2021). The detection of canopy gaps at the 10-m resolution (step 2) was better with this method than with the RADD system (Reiche et al., 2021) and the JRC map (Vancutsem et al., 2021). This is especially due to small

felling gaps, the most important disturbance induced by selective logging in the study area, with 80% and 72% of these missed by the RADD system (Reiche et al., 2021) and the JRC map (Vancutsem et al., 2021), respectively. In both steps, textural indices, which allow for the contextualisation of pixels, were found to be important predictors, as previously demonstrated for the detection of selective logging in the Amazon (Hethcoat et al., 2021). This method was specifically tailored to mimic the organisation of logging activities in Central Africa, where the logging intensity is low (10–15 $m^3.ha^{-1}$; 1–2 $trees.ha^{-1}$) with a limited impact on the canopy for a FSC certified concession (3.88% of loss based on UAV canopy gaps), compared to the impact on 10.8% of the canopy cover in a conventional concession (Ngueguim et al., 2009). Other studies using Sentinel-1 SAR data to monitor logging in the tropics (Ballère et al., 2021; Hethcoat et al., 2021; Reiche et al., 2021), present results for higher logging intensities (> 20 $m^3.ha^{-1}$) or with an MMU that is not adapted to this low logging intensity. Moreover, this is the first time that the logging intensity has been predicted in terms of both the volume and number of cut trees per hectare, which are valuable metrics for the forestry sector (Welsink et al., 2023). This method captured a large range of logging intensities, depending on the size of the observation grid, because, locally, logging can be more intense (up to 9 $trees.ha^{-1}$ and 200 $m^3.ha^{-1}$ for a 100-m grid), or completely absent in some areas. The relationships based on volume were slightly better than those based on the number of trees cut per hectare, whereas the opposite was observed when using UAV canopy gaps. This disparity can be attributed to the fact that the C-band used by Sentinel-1 can penetrate the canopy to some extent (Kellndorfer, 2019) and potentially capture understory disturbances (greater with the volume of the cut tree) compared with UAV images that only reflect canopy openings (more related to the number of cut trees). Indeed, given the relatively homogeneous diameter distribution of the cut trees, a cut tree causes, on average, the same disturbance.

Regarding the assessment and comparison of performance among monitoring studies in tropical forests (Ballère et al., 2021; Carstairs et al., 2022; Hethcoat et al., 2021; Reiche et al., 2021; Vancutsem et al., 2021), the disparity in both the reference datasets and validation approaches raises questions. Reference datasets based on optical satellite data can miss canopy gaps because of cloud cover and spatial resolution (Reiche et al., 2021). Those using forest inventories do not consider all types of logging disturbances, only cut trees (Hethcoat et al., 2021), and log yards and roads (Ballère et al., 2021). In addition, the reference dataset can be locally complete for the disturbances but spatially restricted. For example, Carstairs et al. (2022) used a UAV LiDAR flight covering 310 ha to scale up Gabon, reporting a global accuracy of 99.9%. In this study, an independent dataset (UAV canopy gaps) was used for validation, and its performance was lower than that assessed using the test dataset based on the photo-interpretation of Sentinel-1 SAR data. The independent validation approach proposed in this study is based on robust field data needed for reporting selective logging detection (Hethcoat et al., 2021) and allows an accurate assessment of the method.

In the future, this method used at a single site in Cameroon should be tested on other forest types (Fayolle et al., 2014; Réjou-Méchain et al., 2021) and logging practices such as conventional, artisanal, and illegal logging (Lescuyer et al., 2016), that are practiced in the region. Given that the higher the logging intensity, the better the detection of canopy gaps (Hethcoat et al., 2021), we are confident that this method will also perform well in areas where logging intensity is higher, specifically in conventional concessions which are the most widespread in Central Africa (BAD, 2018). Moreover, logging intensity and the extent of logging concessions are both likely to increase in the coming years with the desire to further industrialise the timber sector in Central Africa (BAD, 2018). In this context, monthly monitoring of selective logging activities using this method will have strong practical applications. Specifically, this method allows the direct estimation of logging intensity on the scale of monthly harvesting or annual cutting areas, both of which are relevant for control by forest administration and certification bodies. In addition, despite their limited local performance, the RADD system (Reiche et al., 2021) and the JRC map (Vancutsem et al., 2021) could already be used to monitor logging intensity in Central Africa, given the promising relationships presented in this study for a grid size of 500–1000 m, while awaiting the extension of this method.

CRediT authorship contribution statement

Chloé Dupuis: Conceptualization, Methodology, Software, Validation, Investigation, Formal analysis, Writing – original draft, Writing – review & editing, Visualization. **Adeline Fayolle:** Conceptualization, Writing – review & editing, Visualization, Supervision. **Jean-François Bastin:** Conceptualization, Software, Writing – review & editing, Visualization. **Nicolas Latte:** Software, Formal analysis. **Philippe Lejeune:** Conceptualization, Methodology, Writing – review & editing, Visualization, Supervision.

Declaration of Competing Interest

The authors declare the following financial interests/personal relationships which may be considered as potential competing interests: Chloe Dupuis reports equipment, drugs, or supplies was provided by Pallisco-CIFM.

Data availability

The authors do not have permission to share data.

Acknowledgments

We thank the Pallisco-CIFM Company for their welcome and logistical support during the field missions as well as for the exchanges and data transmitted during their logging activities. We thank Clément Dupuis for proofreading this manuscript. We thank our financial supporters: the University of Liege; the iDROC project co-financed by the “Programme de Promotion de l’Exploitation Certifiée des Forêts” (PPECF), the FEDER and the Occitanie Region, and implemented by the ASBL Nature+ in collaboration with the companies Sunbirds and TERConsult, and the research organisations Gembloux Agro-Bio Tech, the “Commissariat à l’énergie atomique” (CEA) and CIRAD. We also thank the French Global Environment Facility (FGEF) for the financial support of this study through the DynAfFor (Dynamics of Central African Forests; conventions n°CZZ 1636.01 D and n° CZZ 1636.02 E) and P3FAC (Public-Private Partnership for the Sustainable Management of Central African Forests; convention n°CZZ201.01R) projects.

Appendix A. Supplementary data

Supplementary data to this article can be found online at https://doi.org/10.1016/j.rse.2023.113828.

References

BAD, 2018. Rapport Stratégique Régional - Développement intégré et durable de la filière bois dans le bassin du Congo : Opportunités, Défis et recommmandations Opérationnelles. Vision stratégique et industrialisation de la filière bois en afrique Centrale. Hori.

Ballère, M., Bouvet, A., Mermoz, S., Le Toan, T., Koleck, T., Bedeau, C., André, M., Forestier, E., Frison, P.L., Lardeux, C., 2021. SAR data for tropical forest disturbance alerts in French Guiana: benefit over optical imagery. Remote Sens. Environ. 252 https://doi.org/10.1016/j.rse.2020.112159.

Bullock, E.L., Woodcock, C.E., Souza, C., Olofsson, P., 2020. Satellite-based estimates reveal widespread Forest degradation in the Amazon. Glob. Chang. Biol. 00, 1–14. https://doi.org/10.1111/gcb.15029.

Carstairs, H., Mitchard, E.T.A., McNicol, I., Aquino, C., Chezeaux, E., Ebanega, M.O., Dikongo, A.M., Disney, M., 2022. Sentinel-1 shadows used to quantify canopy loss from selective logging in Gabon. Remote Sens. 14, 4233. https://doi.org/10.3390/rs14174233.

De Wasseige, C., Defourny, P., 2004. Remote sensing of selective logging impact for tropical forest management. For. Ecol. Manag. 188, 161–173. https://doi.org/10.1016/j.foreco.2003.07.035.

Deutscher, J., Gutjahr, K., Perko, R., Raggam, H., Hirschmugl, M., Schardt, M., 2017. Humid tropical forest monitoring with multi-temporal L-, C- and X-band SAR data. In: 2017 9th International Workshop on the Analysis of Multitemporal Remote Sensing Images, MultiTemp 2017. https://doi.org/10.1109/Multi-Temp.2017.8035264.

Durrieu de Madron, L., Fontez, B., Dipapoundji, B., 2000. Dégats d'exploitation et de débardage en fonction de l'intensité d'exploitation en forêt dense humide d'Afrique centrale. Bois Forêt des Trop 264, 57–60.

Esa, 2022. Sentinel-1 SAR user guide [WWW Document]. https://sentinels.copernicus.eu/web/sentinel/user-guides/sentinel-1-sar accessed 10.17.22.

European Commission, 2021. Regulation of the European Parliament and of the council on the making available on the Union market as well as export from the Union of certain commodities and products associated with deforestation and forest degradation and repealing Regulation (EU) No.

Fayolle, A., Picard, N., Doucet, J.L., Swaine, M., Bayol, N., Bénédet, F., Gourlet-Fleury, S., 2014. A new insight in the structure, composition and functioning of central african moist forests. For. Ecol. Manag. 329, 195–205. https://doi.org/10.1016/j.foreco.2014.06.014.

Flores-Anderson, A.I., Herndon, K., Cherrington, E., Thapa, R., Kucera, L., Nguyen, H.Q., Odour, P., Wahome, A., Tenneson, K., Mamane, B., Saah, D., Chishtie, F., Limaye, A., 2019. Introduction and rationale. In: The SAR Handbook - Comprehensive Methodologies for Forest Monitoring and Biomass Estimation, pp. 13–18.

FSC, 2022. Forest Stewardship Council - Africa [WWW Document]. Sub-region Congo Basin. URL (accessed 9.13.22). https://africa.fsc.org/.

Genuer, R., Poggi, J.-M., Tuleau-malot, C., 2014. In: VSURF : un package R pour la sélection de variables à l'aide de forêts aléatoires, in: Journées de Statistique de La SFdS. Rennes, pp. 1–6.

Ghazoul, J., Burivalova, Z., Garcia-Ulloa, J., King, L.A., 2015. Conceptualizing Forest degradation. Trends Ecol. Evol. 30, 622–632. https://doi.org/10.1016/j.tree.2015.08.001.

Hansen, M.C.C., Potapov, P.V., Moore, R., Hancher, M., Tyukavina, A., Thau, D., Stehman, S.V.V., Goetz, S.J.J., Loveland, T.R.R., Kommareddy, A., Egorov, A., Chini, L., Justice, C.O.O., Townshend, J.R.G.R.G., Patapov, P.V., Moore, R., Hancher, M., Tyukavina, A., Thau, D., Stehman, S.V.V., Goetz, S.J.J., Loveland, T.R.R., Kommaredy, A., Egorov, A., Chini, L., Justice, C.O.O., Townshend, J.R.G.R.G., Turubanova, S.A.A., Turubanova, S.A.A., 2013. High-resolution global maps of 21-st-century forest cover change. Science (80-.) 342, 850–854. https://doi.org/10.1126/science.1244693.

Haralick, R.M., Shanmugam, K., Dinstein, I., 1973. Textural features for image classification. IEEE Trans. Syst. Man. Cybern. 3, 610–621.

Hethcoat, M.G., Carreiras, J.M.B., Edwards, D.P., Bryant, R.G., Quegan, S., 2021. Detecting tropical selective logging with C-band SAR data may require a time series approach. Remote Sens. Environ. 259, 112411 https://doi.org/10.1016/j.rse.2021.112411.

Hethcoat, M.G., Edwards, D.P., Carreiras, J.M.B., Bryant, R.G., França, F.M., Quegan, S., 2019. A machine learning approach to map tropical selective logging. Remote Sens. Environ. 221, 569–582. https://doi.org/10.1016/j.rse.2018.11.044.

Hirschmugl, M., Gallaun, H., Dees, M., Datta, P., Deutscher, J., Koutsias, N., Schardt, M., 2017. Methods for mapping Forest disturbance and degradation from optical Earth observation data: a review. Curr. For. Rep. 3, 32–45. https://doi.org/10.1007/s40725-017-0047-2.

Hosonuma, N., Herold, M., De Sy, V., De Fries, R.S., Brockhaus, M., Verchot, L., Angelsen, A., Romijn, E., 2012. An assessment of deforestation and forest degradation drivers in developing countries. Environ. Res. Lett. 7 https://doi.org/10.1088/1748-9326/7/4/044009.

Hubau, W., Lewis, S., Phillips, O., Affum-Baffoe, K., Beeckman, H., Cuní-Sanchez, A., Daniels, A., Ewango, C., Fauset, S., Mukinzi, J., Sheil, D., Sonké, B., Sullivan, M., Sunderland, T., Taedoumg, H., Thomas, S., White, L., Abernethy, K., Adu-Bredu, S., Amani, C., Baker, T., Banin, L., Baya, F., Begne, S., Bennett, A., Benedet, F., Bitariho, R., Bocko, Y., Boeckx, P., Boundja, P., Brienen, R., Brncic, T., Chezeaux, E., Chuyong, G., Clark, C., Collins, M., Comiskey, J., Coomes, D., Dargie, G., de Haulleville, T., Djuikouo, K.M., Doucet, J.-L., Esquivel-Muelbert, A., Feldpausch, T., Fofanah, A., Foli, E., Gilpin, M., Gloor, E., Gonmadje, C., Gourlet-Fleury, S., Hall, J., Hamilton, A., Harris, D., Hart, T., Hockemba, M., Hladik, A., Ifo, S., Jeffery, K., Jucker, T., Yakusu, E., Kearsley, E., Kenfack, D., Koch, A., Leal, M., Levesley, A., Lindsell, J., Lisingo, J., Lopez-Gonzalez, G., Lovett, J., Makana, J.-R., Malhi, Y., Marshall, A., Martin, J., Martin, E., Mbayu, F., Medjibe, V., Mihindou, V., Mitchard, E., Moore, S., Munish, P., Bengone, N., Ojo, L., Ondo, F., Peh, K., Pickavance, G., Poulsen, A., Poulsen, J., Qie, L., Reitsma, J., Rovero, F., Swaine, M., Talbot, J., Taplin, J., Taylor, D., Thomas, D., Toirambe, B., Mukendi, J., Tuagben, D., Umunay, P., Van Der Heijden, G., Verbeeck, H., Vleminckx, J., Willcock, S., Woell, H., Woods, J., Zemagho, L., 2020. Asynchronous carbon sink saturation in African and Amazonian tropical forests. Nature 579, 80–87. https://doi.org/10.1038/s41586-020-2035-0.

Jackson, C.M., Adam, E., 2020. Remote sensing of selective logging in tropical forests: current state and future directions. IForest 13, 286–300. https://doi.org/10.3832/ifor3301-013.

Kellndorfer, J., 2019. Using SAR data for mapping deforestation and forest degradation. In: SAR Handbook: Comprehensive Methodologies for Forest Monitoring and Biomass Estimation.

King, M.D., Platnick, S., Menzel, W.P., Ackerman, S.A., Hubanks, P.A., 2013. Spatial and temporal distribution of clouds observed by MODIS onboard the terra and aqua satellites. IEEE Trans. Geosci. Remote Sens. 51, 3826–3852. https://doi.org/10.1109/TGRS.2012.2227333.

Lescuyer, G., Cerutti, P.O., Tsanga, R., 2016. Contributions of community and individual small-scale logging to sustainable timber management in Cameroon. Int. For. Rev. 18, 40–51. https://doi.org/10.1505/146554816819683744.

Lisein, J., Pierrot-Deseilligny, M., Bonnet, S., Lejeune, P., 2013. A photogrammetric workflow for the creation of a forest canopy height model from small unmanned aerial system imagery. Forests 4, 922–944. https://doi.org/10.3390/f4040922.

Medjibe, V.P., Putz, F.E., Starkey, M.P., Ndouna, A.A., Memiaghe, H.R., 2011. Impacts of selective logging on above-ground forest biomass in the monts de Cristal in Gabon. For. Ecol. Manag. 262, 1799–1806. https://doi.org/10.1016/j.foreco.2011.07.014.

Mermoz, S., Réjou-Méchain, M., Villard, L., Le Toan, T., Rossi, V., Gourlet-Fleury, S., 2015. Decrease of L-band SAR backscatter with biomass of dense forests. Remote Sens. Environ. 159, 307–317. https://doi.org/10.1016/j.rse.2014.12.019.

Mitchell, A.L., Rosenqvist, A., Mora, B., 2017. Current remote sensing approaches to monitoring forest degradation in support of countries measurement, reporting and verification (MRV) systems for REDD+. Carbon Balance Manag. 12 https://doi.org/10.1186/s13021-017-0078-9.

Nagatani, I., Hayashi, M., Watanabe, M., Tadano, T., Watanabe, T., Koyama, C., Shimada, M., 2018. In: Forest early warning system using ALOS-2/PALSAR-2 SCanSAR data (JJ-FAST). Int. Geosci. Remote Sens. Symp. 2018-July, pp. 4181–4184. https://doi.org/10.1109/IGARSS.2018.8517431.

Ngueguim, J., Gatchui, H., Ayobami, S., Orimoogunje, O., 2009. Evaluation of logging impacts on tropical rainforest in eastern Cameroon using remote sensing and GIS techniques. Int. J. Biol. Chem. Sci. 3 https://doi.org/10.4314/ijbcs.v3i4.47163.

Pearson, T.R.H., Brown, S., Murray, L., Sidman, G., 2017. Greenhouse gas emissions from tropical forest degradation: an underestimated source. Carbon Balance Manag. 12, 1–11. https://doi.org/10.1186/s13021-017-0072-2.

Ploton, P., Barbier, N., Couteron, P., Antin, C.M., Ayyappan, N., Balachandran, N., 2017. Remote sensing of environment toward a general tropical forest biomass prediction model from very high resolution optical satellite images. Remote Sens. Environ. 200, 140–153. https://doi.org/10.1016/j.rse.2017.08.001.

Quegan, S., Yu, J.J., 2001. Filtering of multichannel SAR images. IEEE Trans. Geosci. Remote Sens. 39, 2373–2379. https://doi.org/10.1109/36.964973.

Reiche, J., Mullissa, A., Slagter, B., Gou, Y., Tsendbazar, N.E., Odongo-Braun, C., Vollrath, A., Weisse, M.J., Stolle, F., Pickens, A., Donchyts, G., Clinton, N., Gorelick, N., Herold, M., 2021. Forest disturbance alerts for the Congo Basin using Sentinel-1. Environ. Res. Lett. 16 https://doi.org/10.1088/1748-9326/abd0a8.

Réjou-Méchain, M., Mortier, F., Bastin, J.F., Cornu, G., Barbier, N., Bayol, N., Bénédet, F., Bry, X., Dauby, G., Deblauwe, V., Doucet, J.L., Doumenge, C., Fayolle, A., Garcia, C., Kibambe Lubamba, J.P., Loumeto, J.J., Ngomanda, A., Ploton, P., Sonké, B., Trottier, C., Vimal, R., Yongo, O., Pélissier, R., Gourlet-Fleury, S., 2021. Unveiling African rainforest composition and vulnerability to global change. Nature 593, 90–94. https://doi.org/10.1038/s41586-021-03483-6.

Rudant, J.P., Frison, P.L., 2019. Teledetection radar: De l'image d'intensite initiale au choix du mode de calibration des coefficients de diffusion B°, Σ° Γ°. Rev. Fr. Photogramm. Teledetect. 2019-June, 19–28.

Rutishauser, E., Hérault, B., Baraloto, C., Blanc, L., Descroix, L., Sotta, E.D., Ferreira, J., Kanashiro, M., Mazzei, L., D'Oliveira, M.V.N., De Oliveira, L.C., Peña-Claros, M., Putz, F.E., Ruschel, A.R., Rodney, K., Roopsind, A., Shenkin, A., Da Silva, K.E., De Souza, C.R., Toledo, M., Vidal, E., West, T.A.P., Wortel, V., Sist, P., 2015. Rapid tree carbon stock recovery in managed Amazonian forests. Curr. Biol. 25, R787–R788. https://doi.org/10.1016/j.cub.2015.07.034.

Sanchez-Azofeifa, A., Antonio Guzmán, J., Campos, C.A., Castro, S., Garcia-Millan, V., Nightingale, J., Rankine, C., 2017. Twenty-first century remote sensing technologies are revolutionizing the study of tropical forests. Biotropica 49, 604–619. https://doi.org/10.1111/btp.12454.

Scipal, K., Arcioni, M., Chave, J., Dall, J., Fois, F., LeToan, T., Lin, C.C., Papathanassiou, K., Quegan, S., Rocca, F., Saatchi, S., Shugart, H., Ulander, L., Williams, M., 2010. The BIOMASS Mission - an ESA earth explorer candidate to measure the BIOMASS of the Earth's forests. Int. Geosci. Remote Sens. Symp. 52–55 https://doi.org/10.1109/IGARSS.2010.5648979.

Sist, P., Ferreira, F.N., 2007. Sustainability of reduced-impact logging in the Eastern Amazon. For. Ecol. Manage. 243, 199–209. https://doi.org/10.1016/j.foreco.2007.02.014.

Sist, P., Nolan, T., Bertault, J.G., Dykstra, D., 1998. Harvesting intensity versus sustainability in Indonesia. For. Ecol. Manage. 108, 251–260. https://doi.org/10.1016/S0378-1127(98)00228-X.

Tyukavina, A., Hansen, M.C., Potapov, P., Parker, D., Okpa, C., Stehman, S.V., Kommareddy, I., Turubanova, S., 2018. Congo Basin forest loss dominated by increasing smallholder clearing. Sci. Adv. 4, 1–12. https://doi.org/10.1126/sciadv.aat2993.

Vancutsem, C., Achard, F., Pekel, J.F., Vieilledent, G., Carboni, S., Simonetti, D., Gallego, J., Aragão, L.E.O.C., Nasi, R., 2021. Long-term (1990–2019) monitoring of forest cover changes in the humid tropics. Sci. Adv. 7, 1–22. https://doi.org/10.1126/sciadv.abe1603.

Vollrath, A., Mullissa, A., Reiche, J., 2020. Angular-based radiometric slope correction for Sentinel-1 on Google Earth Engine. Remote Sens. 12, 1–14. https://doi.org/10.3390/rs12111867.

Watanabe, M., Koyama, C.N., Hayashi, M., Nagatani, I., Shimada, M., 2018. Early-stage deforestation detection in the tropics with L-band SAR. IEEE JSel. Top. Appl. Earth Obs. Remote Sens 11, 2127–2133. https://doi.org/10.1109/JSTARS.2018.2810857.

Welsink, A.J., Reiche, J., de Sy, V., Carter, S., Slagter, B., Suarez, D.R., Batros, B., Peña-Claros, M., Herold, M., 2023. Towards the use of satellite-based tropical forest disturbance alerts to assess selective logging intensities. Environ. Res. Lett. 18 https://doi.org/10.1088/1748-9326/acd018.